A Platinum Open Access Journal for Organic Chemistry

Paper

Free to Authors and Readers | DOAJ Seal | *Arkivoc* **2021**, part viii, 0-0

Synthesis and DFT studies of novel aminoimidazodipyridines using 2-(3*H*-imidazo[4,5-*b*]pyrid-2-yl)acetonitrile as an efficient key precursor

Ahmed F. Darweesh,[a] Nesma A. Abd El-Fatah,[a] Samir A. Abdel-Latif,[b] Ismail A. Abdelhamid,[a]* Ahmed H. M. Elwahy[a]* and Mostafa E. Salem[a]

[a]*Department of Chemistry, Faculty of Science, Cairo University, Giza 12613, Egypt*
[b]*Department of Chemistry, Faculty of Science, Helwan University, Cairo 11795, Egypt*
Email: ismail_shafy@yahoo.com, aelwahy@hotmail.com

Received 11-10-2020 **Accepted** 01-20-2021 **Published on line** 02-08-2021

Abstract

Novel 9-aminoimidazo[1,2-*a*:5,4-*b*']dipyridine-6,8-dicarbonitriles were prepared *via* the Michael addition reaction of readily accessible 2-(3*H*-imidazo[4,5-*b*]pyrid-2-yl)acetonitrile with arylidenemalononitriles. The regioselectivity of the reaction was supported by theoretical calculations at the DFT level. In contrast, the reaction of the appropriate bis-arylidenemalononitrile with 2-(3*H*-imidazo[4,5-*b*]pyrid-2-yl)acetonitrile under similar reaction conditions gave the corresponding bis[2-(3*H*-imidazo[4,5-*b*]pyrid-2-yl)acrylonitriles].

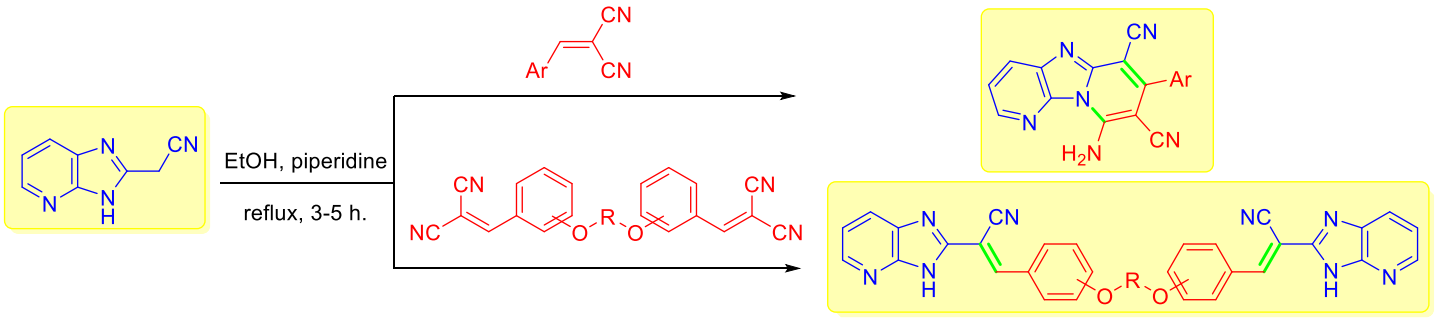

Keywords: 2-(3*H*-imidazo[4,5-*b*]pyrid-2-yl)acetonitrile, 9-aminoimidazo[1,2-*a*:5,4-*b*']dipyridine-6,8-dicarbonitrile, arylidenemalononitriles, bis[2-(3*H*-imidazo[4,5-*b*]pyrid-2-yl)acrylonitriles], DFT studies.

Introduction

Imidazo[4,5-*b*]pyridines are important classes of heterocyclic compounds that possess diverse pharmacological properties including anticancer,[1] antimicrobial,[2] anti-inflammatory,[3] and antiviral activities.[4,5] Moreover, N-fused polyheterocycles display also a wide range of biological activities.[6] In particular, imidazo[1,2-*a*:5,4-*b*']dipyridines exhibit interesting anticancer[7] and antiviral[8] activities. Some examples of biologically active compounds containing an imidazo[1,2-*a*:5,4-*b*']dipyridine such as (CF02334) **1**, a selective inhibitor of the cytopathic effect (CPE) caused by bovine viral diarrhea[8] and anti-human prostate cancer **2**[7] are outlined in Figure 1. In addition, the development of simple and efficient synthetic routes to novel heterocyclic compounds represents a great challenge in organic synthesis. In this respect, the Michael addition reaction has attracted much attention in the last decades as an effective strategy for the synthesis of heterocycles and their fused derivatives under mild reaction conditions.[9,10] Moreover, due to their promising nonlinearoptical (NLO) properties, imidazo[1,2-*a*]pyridine and their corresponding fused derivatives have a diverse range of applications in material chemistry. In this respect, many of these derivatives have been used as multiple fluorescent chemosensors, in an electron transport layer of an organic light emitting device, as biomarkers of hypoxic tumor cells, and as a receptor in fluorescent high-affinity ligand in dopamine D3.[11–14]

In connection with the increasing interest of adoption of new synthetic methods in drug discovery, and in continuation to our recent applications of carbon-Michael[15–18] as well as aza-Michael[16] addition reactions as powerful tools for the synthesis of nitrogen containing heterocycles and their corresponding bis-heterocycles,[15,17,19–26] we report herein our investigation on the reactivity of 2-(3*H*-imidazo[4,5-*b*]pyrid-2-yl)acetonitrile towards arylidenemalononitriles and bis-arylidenemalononitriles aiming at synthesizing novel mono- and bis-imidazo[1,2-*a*:5,4-*b'*]dipyridine-6,8-dicarbonitriles. In addition, a theoretical density functional theory (DFT) study aims to determine the more stable regioisomer of the two possible expected isomeric products from the mentioned reactions as well as to investigate the efficacy of the target compounds as suitable candidate for NLO material.

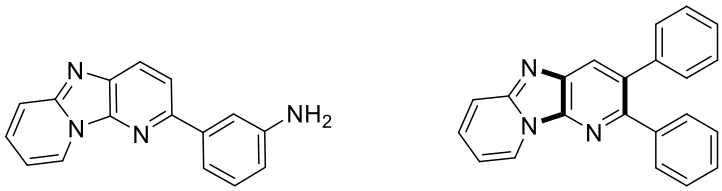

1 **2**

Figure 1. Some examples of biologically active compounds containing imidazo[1,2-*a*:5,4-*b*']dipyridines.

Results and Discussion

Synthesis

Previously, various methods have been reported for the synthesis of imidazo[1,2-*a*:5,4-*b*']dipyridines. Most of these methods depend mainly on the formation of 3-aminoimidazo[1,2-*a*]pyridines followed by their reaction with the appropriate reagents. In this respect, Takeda *et al*.[27] synthesized imidazodipyridines **5** by the reaction of 3-aminoimidazo[1,2-*a*]pyridine **3** (R = H) with 2-chloroacrylonitrile **4** in nitrobenzene in the presence of

$AlCl_3$. Moreover, Desbois *et al*.[28] synthesized imidazo[1,2-*a*:5,4-*b*']dipyridines **6** *via* the reaction of 3-amino-2-formylimidazo[1,2-*a*]pyridine **3** (R = CHO) with various aldehydes or ketones by Friedländer's method (Scheme 1).

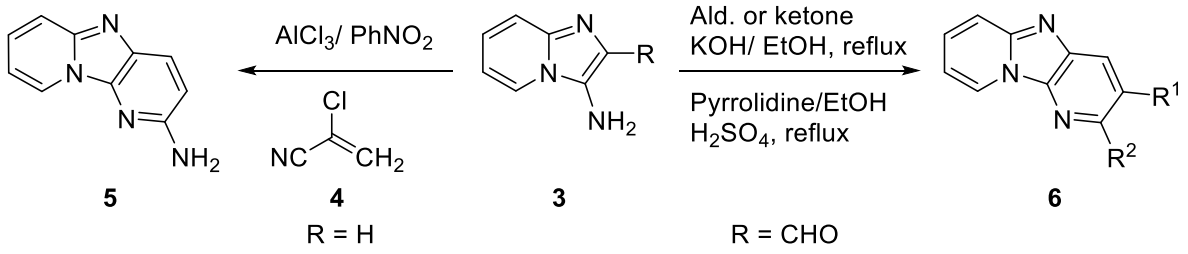

Scheme 1. Reported Methods for the synthesis of imidazodipyridines **5** and **6**.

Li *et al*.[7] and Zhang *et al*.[29] also reported on the utility of some imidazo[1,2-*a*]pyridin-3-amines as precursors for the synthesis of imidazo[1,2-*a*:5,4-*b*']dipyridines.

In searching for an expedient strategy for synthesis of imidazodipyridines, our attention focused on 2-(3*H*-imidazo[4,5-*b*]pyrid-2-yl)acetonitrile (**10**) as a precursor. Compound **10** was prepared *via* the solvent-free reaction of pyridine-2,3-diamine (**7**) with ethyl cyanoacetate (**8**) in an oil bath at 180-190 °C for 30 minutes (Scheme 2). The structure of compound **10** was supported by the presence of FTIR bands at 3410 and 2252 cm^{-1} characteristic for *v*(N-H) and *v*(C≡N) groups, respectively. The ^{1}H NMR spectrum of compound **10** reveals the methylene group and the NH protons at δ 4.42 and 13.18, respectively. The data agreed with that previously reported for compound **10**.[30,31]

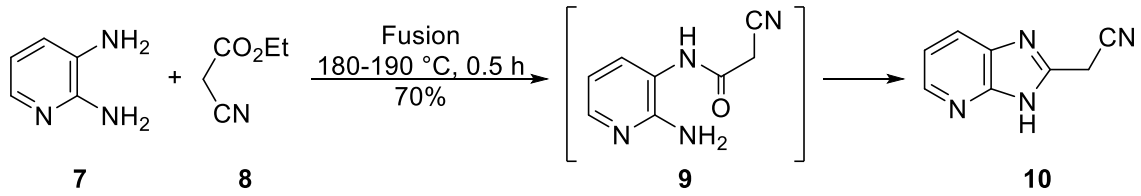

Scheme 2. Synthesis of 2-(3*H*-imidazo[4,5-*b*]pyrid-2-yl)acetonitrile **10**.

The reactivity of compound **10** towards substituted cinnamonitriles was then investigated. Compound **10** (a Michael donor) has two nucleophilic centers (NH group and CH_2) at which the Michael addition to the Michael acceptor **11** can initiate. Thus, two regioisomeric products are possible by the reaction of compound **10** with the activated double bond reagents **11** *via* routes A and B (Schemes 3 & 4). Route A involves the initial nucleophilic addition of CH_2 of compound **10** to β-carbon of the activated double bond of **11** followed by cyclization that involves the NH group to afford 9-amino-7-arylimidazo[1,2-*a*:5,4-*b'*]dipyridine-6,8-dicarbonitrile **12** through intermediates **14** and **15** (Scheme 4). Route B encompasses the initial addition of the NH group of the compound **10** to the activated double bond of **11** followed by cyclization involving CH_2 of **10** to give 7-amino-9-arylimidazo[1,2-*a*:5,4-*b'*]dipyridine-6,8-dicarbonitrile **13** through intermediates **16** and **17** (Scheme 4). The structures of the expected products **12** or **13** could not be determined based on spectral analyses as both of them give similar data. For example, the IR spectrum of the compound produced from the reaction of **10** with **11a** showed the presence of amino group at *v*(N-H) 3456 and 3317 cm^{-1} as well as

characteristic nitrile band at *ν*(C≡N) 2214 cm^{-1}. Its ^1H NMR spectrum revealed the amino group at *δ* 8.89 as a broad signal. Unfortunately, these data can agree with both structures **12** and **13**.

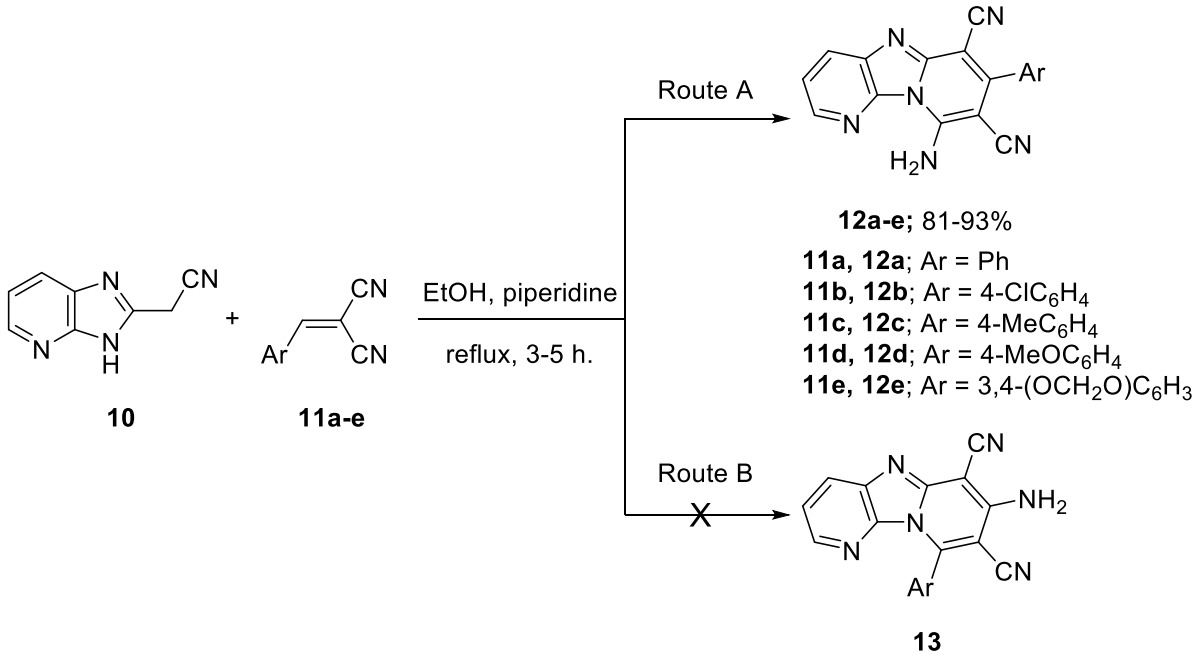

Scheme 3. Synthesis of compounds **6a-e** *via* reaction of **4** with cinnamonitriles.

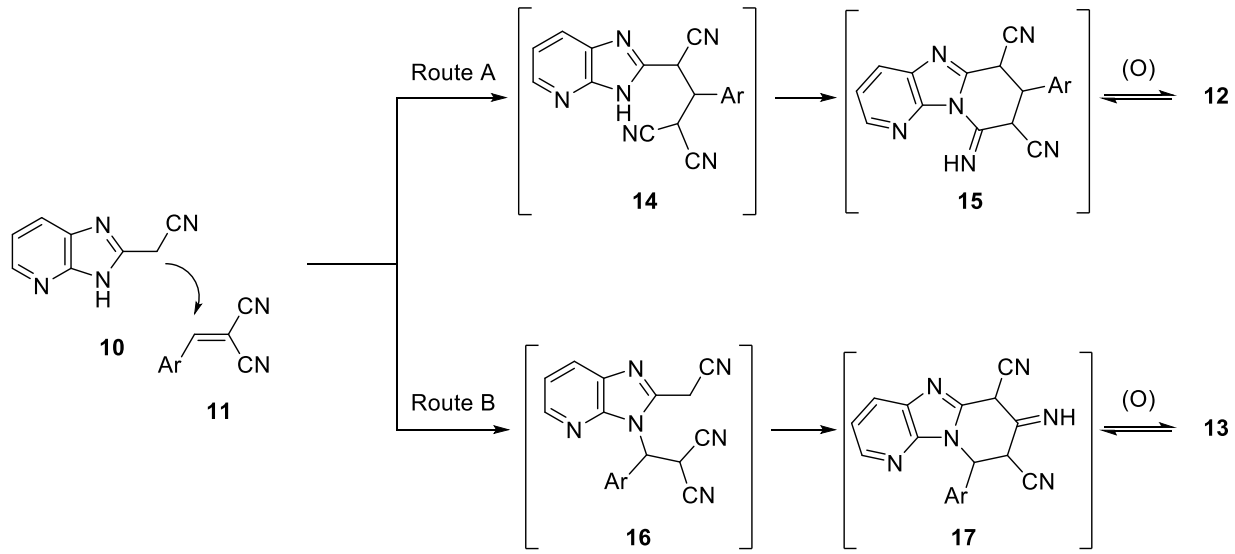

Scheme 4. Expected routes (A and B) for the formation of regioisomeric products **12** and **13**.

Route A that affords compounds **12** was approved based on literature similarities[32,33] that indicated the superiority of the nucleophilicity of CH_2 over NH group. Further support for the formation of compound **12a** was provided by an alternative synthesis *via* a three component reaction of 2-(3*H*-imidazo[4,5-*b*]pyrid-2-yl)acetonitrile **10** with both benzaldehyde (**18**) and malononitrile (**19**) in EtOH heated at reflux in the presence of catalytic piperidine (Scheme 6, Method B). Moreover, compound **12a** was also obtained *via* the reaction of malononitrile (**19**) with a preheated mixture of benzaldehyde (**18**) and 2-(3*H*-imidazo[4,5-*b*]pyrid-2-yl)acetonitrile **10**. In support of this viewpoint, we also isolated the Knoevenagel condensation product 2-(3*H*-

imidazo[4,5-*b*]pyrid-2-yl)-3-phenylacrylonitrile (**20**) (Scheme 5, method C). The formation of **12a** from the reaction of **20** with **19**, with identical physical and spectral data with that prepared from the reaction of **10** and **11a**, supports the reaction proceeded *via* route A and not *via* route B.

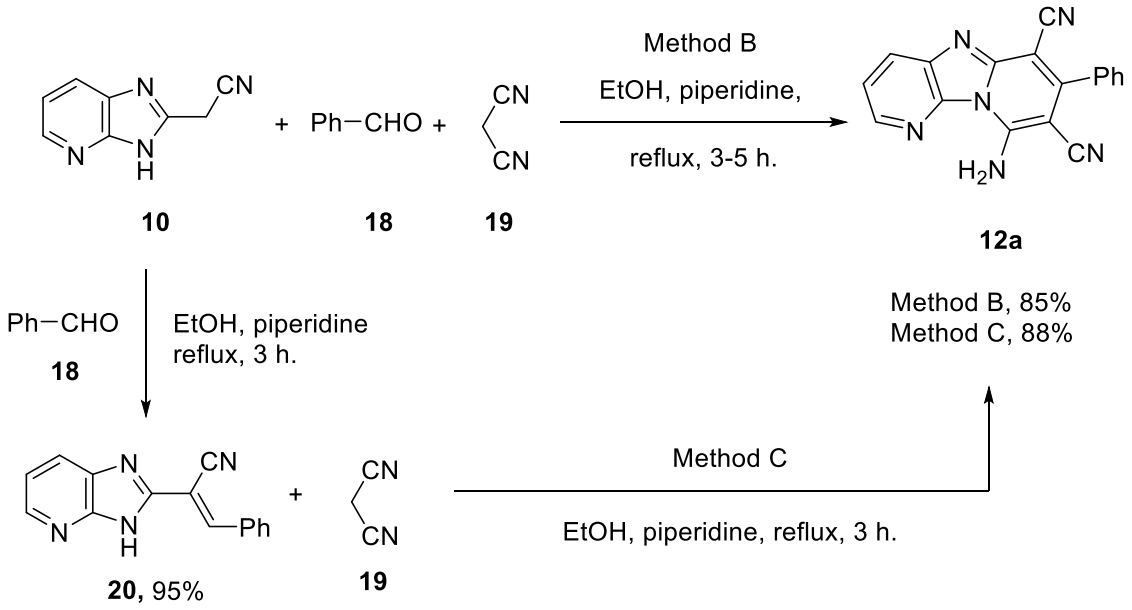

Scheme 5. Alternative methods for the synthesis of compound **12a**.

The regioselective formation of **12** was also supported by theoretical calculations at DFT level (cf. Molecular orbital calculations).

In searching for the optimal reaction conditions, the reaction was carried out in different solvents as well as in the presence of a variety of bases. Firstly, we tried EtOH as a solvent and DABCO, pyridine, KOH, TEA and piperidine as bases. Among the different bases, the use of piperidine gave the cleanest products and best yields. The reaction was also examined in different solvents including dioxane, dichloromethane, acetonitrile, water and DMF heated at reflux in each case. The reaction proceeded in most solvents but with different degrees of conversion; EtOH was the best solvent in terms of reaction time and yield. The reactions were completed in 3-5 h, while prolonged heating did not improve the reaction yield. On the other hand, no traces of products were obtained at room temperature. The reactivity of compound **10** towards heteromethylenemalononitriles was also investigated aiming at synthesizing novel imidazo[1,2-*a*:5,4-*b'*]dipyridines which are linked to heterocyclic moieties at position 7. Thus reaction of **10** with each of 2-[(1,3-diphenylpyrazol-4-yl)methylene]malononitrile (**21a**) and 2-{[1-phenyl-3-(thien-2-yl)-pyrazol-4-yl]methylene}-malononitrile (**21b**) afforded 9-amino-7-arylimidazo[1,2-*a*:5,4-*b'*]dipyridine-6,8-dicarbonitrile **22a** and **22b**, respectively, in good yields (Scheme 6).

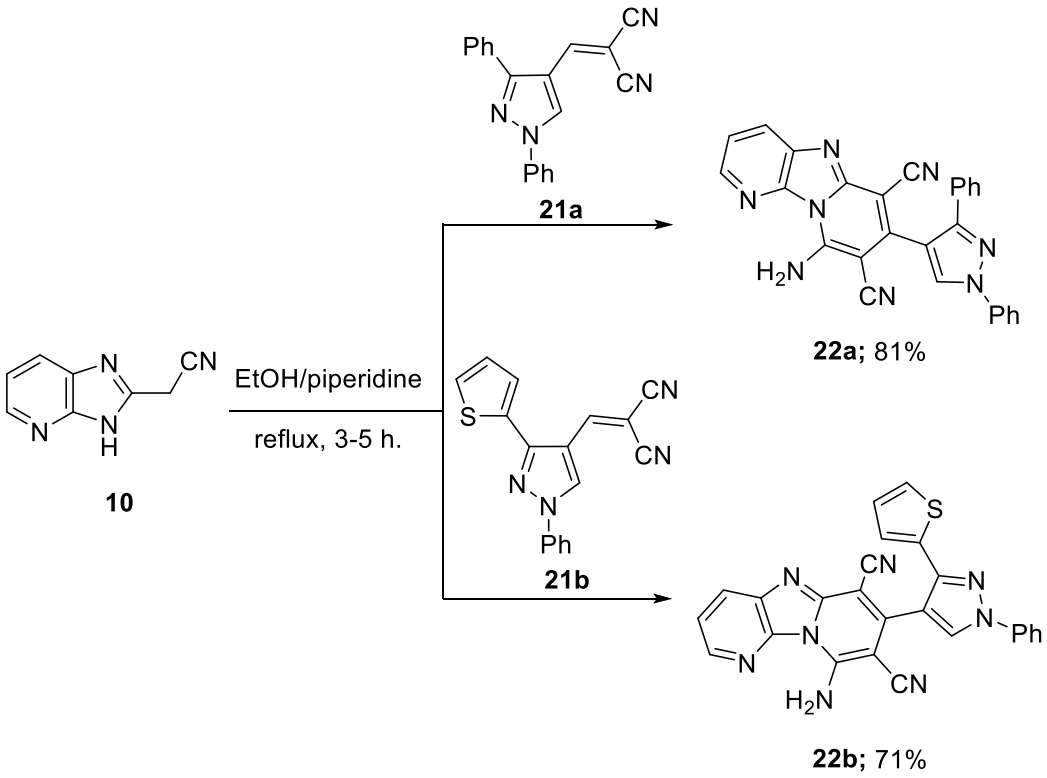

Scheme 6. Synthesis of imidazo[1,2-*a*:5,4-*b'*]dipyridines **22a** and **22b** *via* reaction of compound **10** with heteromethylenemalononitriles.

Our study was extended to investigate the reactivity of 2-(3*H*-imidazo[4,5-*b*]pyrid-2-yl)acetonitrile (**10**) towards bis-arylidenemalononitrile **23** in a trial to prepare bis-9-amino-7-arylimidazo[1,2-*a*:5,4-*b'*]dipyridine-6,8-dicarbonitriles **24**. Unfortunately, Michael addition of two equivalents of 2-(3*H*-imidazo[4,5-*b*]pyrid-2-yl)acetonitrile (**10**) to bis-arylidenemalononitriles did not lead to the formation of **24**. Instead the reaction gave bis[2-(3*H*-imidazo[4,5-*b*]pyrid-2-yl)acrylonitriles] **25a-d** (Scheme 7). Compounds **25** are assumed to form *via* the initial formation of the Michael adducts **26** which then decompose to afford **25** *via* elimination of malononitrile (Scheme 8). A similar pathway has been reported.[34] The structures of compounds **25a-d** were supported by comparison of their physical data with authentic samples prepared from the reaction of one equivalent of bis-aldehydes **27** with two equivalents of 2-(3*H*-imidazo[4,5-*b*]pyrid-2-yl)acetonitrile (**10**) in EtOH in the presence of catalytic piperidine (Scheme 9). The constitutions of compounds **25** were established based on spectral data. Thus, the ^{1}H NMR spectrum of compound **25a** as a representative example revealed two singlet signals at δ 4.63 and 8.59 for the OCH_2 groups and the ylidene H-atoms, respectively. Moreover, it revealed the NH group as broad singlet at 13.63 ppm.

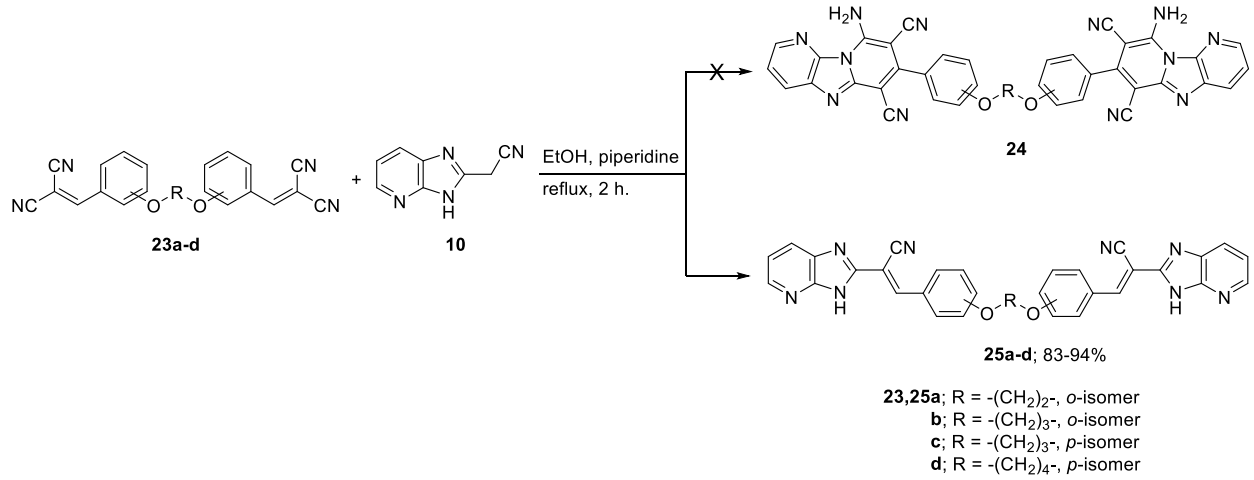

Scheme 7. Attempted synthesis of bis-9-amino-7-arylimidazo[1,2-*a*:5,4-*b'*]dipyridine-6,8-dicarbonitriles **24** *via* reaction of **10** with bis-arylidenemalononitrile **23**.

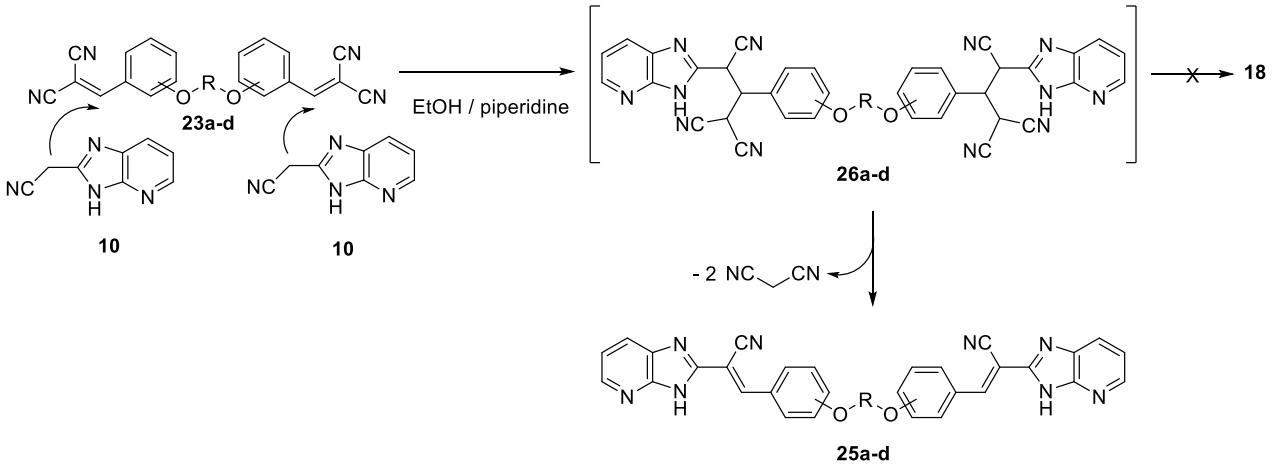

Scheme 8. Plausible mechanism for the formation of **25a-d** *via* reaction of **10** with bis-arylidenemalononitrile **23**.

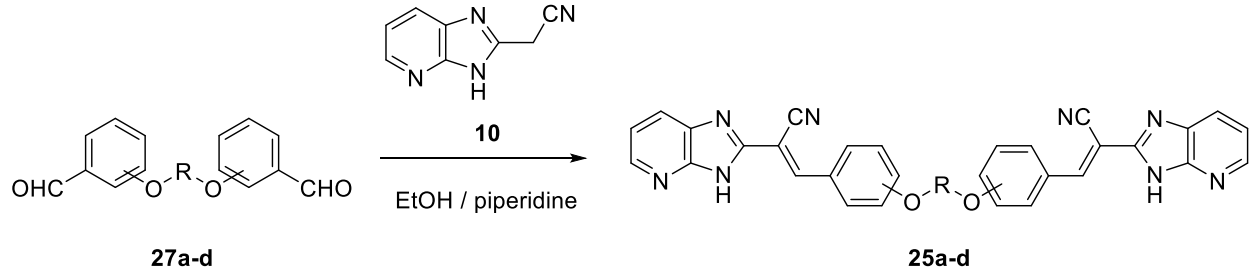

Scheme 9. Synthesis of compounds **25a-d** by the reaction of one equivalent of bis-aldehydes **27** with two equivalents of **10**.

Theoretical calculations

Geometry of compounds 12 and 13

Geometry structures of the expected products **12** and **13** and their intermediates **14** and **16** were optimized at the B3LYP/6-311G** level and the results are given in Table 1. The reaction of **10** with **11** can lead to the formation of the regioisomer **12**, via intermediate **14** through the attack of the active CH_2 of **10** (C14) on CH groups of **11** (C12). On the other hand, the regioisomer **13** can arise *via* initial attack of NH of **10** on CH of **11** to give intermediate **16** as seen in Fig. 2 (cf. supporting information). The energy of regioisomer **13** was 7.15 kcal/mol higher than that of **12**, i.e., the structure of **12** was more stable. Also, the intermediate **16** has energy of 5.52 kcal/mol higher than that of **14**. Therefore, this study supports the regioselective formation of **12** from the reaction of **10** with **11**. The planarity of **12** can be estimated from the values of the dihedral angles. Compound **12** has a non-planar structure where the phenyl ring rotates out of the plane. This is can be indicated from the dihedral angles of the phenyl ring attached to C13-C24, especially the angles (<C13-C11-C12-N17), (<C13-C14-C16-N18) and (<C11-C13-C24-C29) which are -176.879°, -179.389° and 123.976° (Table 1, cf. supporting information). Where these angles are far from 0° or 180°. This also can be verified from the bond angel (<C14-C13-C24) which has the value of 119.117° (Table 1).

Ground state properties and Global reactivity descriptors

The energy difference between the HOMO and LUMO, E_g, of compounds **10**, **11** and **12** occur in the range 5.28-3.32 eV. The energy gap of compound **10** is the maximum (5.28 eV) while that for compound **12** has the minimum (3.32 eV) value (Table 2). As a result, charge transfer and polarization can easily occur with more reactivity within **12** than **10** and **11**. The electronegativity, χ, chemical hardness, η, global softness, S, chemical potential, π, were calculated using HOMO and LUMO energies and were recorded in Table 2, Fig. 3 (cf. supporting information). Compound **10** has the lowest η and maximum S value which means that the charge transfer occurs easily in this compound and it has a lower chemical hardness. Large E_g gaps are representative of the hardness of the molecule, while smaller E_g gaps are representative for soft and reactive molecules. The accumulated data in Table 2 showed that the HOMO of **12** is less stable than that of the other compounds and has lower IP value. The electron affinities values are of the order: **10** < **12** < **11**. The processed reactivity parameters are shown in Table 2 which revealed that compound **10** has the lowest η and minimum S values. This indicated that it has lower chemical hardness. The 3-D distribution of frontier MOs, HOMO and LUMO of **10**, **11** and **12** are presented in Fig. 2. The calculated values of E_{HOMO} and E_{LUMO} of **12** are -6.1690 and -2.8478 eV, respectively, thus the energy gap value E_g is 3.3212 eV. It can be regarded from Fig. 3 that the HOMO and LUMO of **12** are mainly allocated over the whole molecule. The partial frontier molecular orbital compositions and the energy levels of **12** in the ground state are recorded in Table 2 and Fig. 3.

Table 2. Total energy, energy of HOMO and LUMO, energy gap, of **10**, **11, 12, 13, 14** and **16** usingB3LYP/6-311G**

Parameter	**10**	**11**	**12**	**13**	**14**	**16**
E_T, eV	-14350	-13436	-27762	-27744	-27771	-27771
E_{HOMO}, eV	-6.7891	-7.3929	-6.1690	-5.9867	-6.8653	-6.9795
E_{LUMO}, eV	-1.5150	-3.0926	-2.8478	-3.2776	-1.7789	-1.8170
E_g, eV	5.2741	4.3003	3.3212	2.7091	5.0864	5.1625

The frequency calculations for compound **12a** (Figure 4, cf. supporting information) were performed using B3LYP/6-31G(d,p). The data obtained are comparable with that theoretically calculated (Exp. 3456, 3317, 2214; Calc. 3470, 3240, 2212 cm^{-1}) cf. experimental section. TD-DFT calculations for compound **12a** (Figure 5, cf. supporting information) were brought out at the same level of theory [B3LYP/6-31G(d,p)] to clarify the origin of the electronic spectra, using the polarizable continuum solvation method, PCM, PCM-TD-DFT. The theoretical spectrum of **12a** is characterized by five bands at 361 (3.4316 eV), 308 (4.0224 eV), 286 (4.3248 eV), 262 (4.7280 eV) and 245 nm (5.0405 eV). Theoretical IR and UV spectra of **12a** using B3LYP6-31G(d,p) are mentioned in supplementary material.

Non-linear optical properties (NLO)

The circulation of the atomic charges in the chelates is also valuable in the determination of the magnitude and direction of the moment vector which depends on the centers of negative and positive charges. The dipole moment, the mean polarizability, the anisotropy of the polarizability and the first-order hyperpolarizability for compounds **10**, **11** and **12** were calculated using the same level and the obtained values are tabulated in Table 3. The table also includes the experimental values of urea. The considered dipole moment values of **10**, **11** and **12** in the gas phase are 4.4076, 6.6808 and 5.3942 D, respectively. The analyzed values of the polarizability of **10**, **11** and **12** have the range 1.09-7.02×10^{-24} (esu). Compound **11** has the lowest calculated value and **12** has 7.02×10^{-24}. Compared with urea[35] as a reference substance, all the studied chelates have higher polarizability and first-order hyperpolarizability. The polarizabilities and first-order hyperpolarizabilities are reported in atomic units (a.u.), the calculated values have been changed into electrostatic units (esu) using conversion factor of 0.1482×10^{-24} esu for α and 8.6393×10^{-33} esu for β. Urea is used as standard example in non-linear optical studies. In this study, urea is chosen as a reference material as there were no experimental values of NLO properties for the new derivatives. The extent of the molecular hyperpolarizability (<β>) is one of the key factors in non-linear optical system. The calculated (<β>) values for compounds **10**, **11** and **12** are ~6, ~60, and ~6, times greater than that of urea, respectively. Therefore, all the studied compounds reveal considerable polarizability and first-order hyperpolarizability and are projected to be successful encouraged for NLO materials.

Conclusions

We developed a simple and an efficient method for the preparation of novel 9-aminoimidazo[1,2-*a*:5,4-*b*']dipyridine-6,8-dicarbonitriles *via* the Michael addition reaction that involves 2-(3*H*-Imidazo[4,5-*b*]pyrid-2-yl)acetonitrile (as Michael donor) and the appropriate arylidenemalononitriles (as Michael acceptor). Also, we managed to synthesize bis[2-(3*H*-imidazo[4,5-*b*]pyrid-2-yl)acrylonitriles] through the reaction of 2-(3*H*-imidazo[4,5-*b*]pyrid-2-yl)acetonitrile with bis-arylidenemalononitriles under similar reaction conditions. The theoretical calculations were carried out using Gaussian 09 W package with Gauss View 5. The analysis includes bond lengths, bond angles, molecular electrostatic potential maps, description of the important frontier molecular orbital surfaces of the compounds. The optimized molecular structure of the compounds was obtained at B3LYP/6-311G**. The regioisomer **13** has higher energy than that of **12**. This gives further confirmation for the formation of the more stable regioisomer **12**. The polarizability and hyperpolarizabilities parameters of the compounds indicated that they are suitable candidate for NLO material.

Experimental Section

General. Melting points were determined in open glass capillaries with a Gallenkamp apparatus. The infrared spectra were recorded in potassium bromide disks on a Pye Unicam SP 3-300 and Shimaduz FTIR 8101 PC infrared spectrophotometer. NMR spectra were recorded using a Varian Mercury VXR-300 NMR spectrometer or Bruker Ultrashield 400 MHz or Ascend 400 MHz (^{1}H: 300 or 400 MHz, ^{13}C: 75 or 100.6 MHz) instruments using DMSO-d_6 as solvent. Mass spectra (EI) were obtained at 70 eV using a type Shimadzu GCMQP 1000 EX Spectrometer. Elemental analyses were performed on a Perkin-Elmer 240 microanalyser at the Micro analytical Center of Cairo University. Compounds **10**[36], **11**[37], **23a-d**[38] and **27a-d**[38] were prepared according to the literature.

General procedure for the synthesis of 9-amino-7-substituted imidazo[1,2-*a*:5,4-*b*']dipyridine-6,8-dicarbonitrile 12a-e and 22a,b

Method A. To a mixture of appropriate arylidene malononitrile **11a-e**, **21a** or **21b** (1 mmol) and 2-(3*H*-imidazo[4,5-*b*]pyrid-2-yl)acetonitrile (**10**) (1 mmol, 158 mg) in absolute EtOH (15 mL) was added piperidine (1 mmol, 110 μL), and the mixture was heated at reflux for 3-5 h. The crude solid was isolated and recrystallized from EtOH/DMF to give **12a-e** and **22a,b**, respectively.

For compound 12a:

Method B. To a mixture of benzaldehyde (**18**) (1 mmol, 106 mg), malononitrile (**19**) (1 mmol, 66 mg) and 2-(3*H*-imidazo[4,5-*b*]pyrid-2-yl)acetonitrile (**10**) (1 mmol, 158 mg) in absolute EtOH (25 mL) was added piperidine (1 mmol, 110 μL), and the reaction mixture was heated at reflux for 5 h. The crude solid was isolated and recrystallized from DMF/EtOH (25:75) to give **12a**.

Method C. A mixture of 2-(3*H*-imidazo[4,5-*b*]pyrid-2-yl)-3-phenylacrylonitrile (**20**) (1 mmol, 246 mg) and malononitrile (**19**) (1 mmol, 66 mg) in absolute EtOH (15 mL) was added piperidine (1 mmol, 110 μL), and the mixture was heated at reflux for 3 h. The crude solid was isolated and recrystallized from DMF/EtOH (25:75) to give **12a**.

9-Amino-7-phenylimidazo[1,2-*a*:5,4-*b*']dipyridine-6,8-dicarbonitrile (12a). Brown crystals, (method A (288 mg, 93%); method B (263 mg, 85%); method C (273 mg, 88%); mp > 300 °C; IR (KBr) *v* (Exp. 3456, 3317, 2214; Calc. 3470, 3240, 2212) cm^{-1}; ^{1}H NMR (400 MHz, DMSO-d_6) δ 7.42-7.46 (m, 1H, pyridine-H), 7.49-7.62 (m, 5H, ArH), 8.70-8.71 (m, 1H, pyridine-H), 8.89 (br. s, 2H, NH_2), 9.00-9.02 (m, 1H, pyridineH); ^{13}C NMR (100 MHz, DMSO-d_6) δ 78.7, 115.9, 116.2, 117.2, 121.8, 123.6, 129.2, 130.7, 135.2, 137.8, 142.1, 148.4, 149.7, 152.8, 154.6, 156.6; MS *m/z* (%) 310 (M^+). Anal. Calcd for $C_{18}H_{10}N_6$: C, 69.67; H, 3.25; N, 27.08. Found: C, 69.52; H, 3.07; N, 26.97%.

9-Amino-7-(4-chlorophenyl)imidazo[1,2-*a*:5,4-*b*']dipyridine-6,8-dicarbonitrile (12b). Brown crystals (279 mg, 81%); mp > 300 °C; IR (KBr) *v* 3454, 3317, 2214 cm^{-1}; ^{1}H NMR (400 MHz, DMSO-d_6) δ 7.43-7.46 (m, 1H, pyridine-H), 7.64-7.72 (m, 5H, ArH), 8.69-8.71 (m, 1H, pyridine-H), 8.93 (br. s, 2H, NH_2), 9.00-9.03 (m, 1H, pyridine-H); ^{13}C NMR (100 MHz, DMSO-d_6) δ 79.0, 115.9, 116.1, 117.3, 121.8, 123.6, 129.3, 131.1, 134.1, 135.6, 144.4, 148.5, 149.6, 152.8, 153.3, 156.6; MS *m/z* (%) 344 (M^+). Anal. Calcd for $C_{18}H_9ClN_6$: C, 62.71; H, 2.63; N, 24.38. Found: C, 62.46; H, 2.44; N, 24.28%.

9-Amino-7-(*p*-tolyl)imidazo[1,2-*a*:5,4-*b*']dipyridine-6,8-dicarbonitrile (12c). Pale brown crystals (282 mg, 87%); mp > 300 °C; IR (KBr) *v* 3456, 3317, 2214 cm^{-1}; ^{1}H NMR (400 MHz, DMSO-d_6) δ 2.44 (s, 3H, CH_3), 7.41-7.52 (m, 5H, ArH & pyridine-H), 8.68-8.69 (m, 1H, pyridine-H), 8.82 (br. s, 2H, NH_2), 8.99-9.02 (m, 1H, pyridine-H); ^{13}C NMR (100 MHz, DMSO-d_6) δ 21.4, 79.0, 116.2, 116.4, 117.1, 121.9, 123.5, 129.1, 129.7, 132.3, 140.5,

148.3, 149.9, 153.0, 154.6, 156.7; MS *m/z* (%) 324 (M^+). Anal. Calcd for $C_{19}H_{12}N_6$: C, 70.36; H, 3.73; N, 25.91. Found: C, 70.15; H, 3.55; N, 25.79%.

9-Amino-7-(4-methoxyphenyl)imidazo[1,2-*a*:5,4-*b*']dipyridine-6,8-dicarbonitrile (12d). Pale brown crystals (309 mg, 91%); mp > 300 °C; IR (KBr) *v* 3456, 3294, 2214 cm^{-1}; ^1H NMR (400 MHz, DMSO-d_6) δ 3.88 (s, 3H, OCH_3), 7.17 (d, 2H, ArH, *J* 8.8 Hz), 7.42-7.45 (m, 1H, pyridine-H), 7.58 (d, 2H, ArH, *J* 8.4 Hz), 8.69-8.70 (m, 1H, pyridine-H), 8.81 (br. s, 2H, NH_2), 8.99-9.01 (m, 1H, pyridine-H); ^{13}C NMR (100 MHz, DMSO-d_6) δ 55.7, 79.0, 114.5, 116.2, 116.4, 117.1, 121.8, 123.6, 127.1, 130.9, 148.0, 149.9, 152.9, 154.3, 156.7, 161.2; MS *m/z* (%) 340 (M^+). Anal. Calcd for $C_{19}H_{12}N_6O$: C, 67.05; H, 3.55; N, 24.69. Found: C, 66.89; H, 3.32; N, 24.50%.

9-Amino-7-(benzo[*d*][1,3]dioxol-5-yl)imidazo[1,2-*a*:5,4-*b*']dipyridine-6,8-dicarbonitrile (12e). Brown crystals (315 mg, 89%); mp > 300 °C; IR (KBr) *v* 3457, 3284, 2214 cm^{-1}; ^1H NMR (400 MHz, DMSO-d_6) δ 6.19 (s, 2H, OCH_2O), 7.10-7.21 (m, 3H, ArH), 7.41-7.44 (m, 1H, pyridine-H), 8.68-8.69 (m, 1H, pyridine-H), 8.83 (br. s, 2H, NH_2), 8.98-9.01 (m, 1H, pyridine-H); ^{13}C NMR (100 MHz, DMSO-d_6) δ 78.9, 102.3, 109.0, 109.5, 116.1, 116.4, 117.1, 121.8, 123.5, 123.7, 128.6, 147.7, 148.4, 149.3, 149.8, 152.8, 154.1, 156.7; MS *m/z* (%) 354 (M^+). Anal. Calcd for $C_{19}H_{10}N_6O_2$: C, 64.41; H, 2.84; N, 23.72. Found: C, 64.25; H, 2.64; N, 23.58%.

9-Amino-7-(1,3-diphenyl-1*H*-pyrazol-4-yl)imidazo[1,2-*a*:5,4-*b*']dipyridine-6,8-dicarbonitrile (22a). Yellow crystals (366 mg, 81%); mp > 300 °C; IR (KBr) *v* 3448, 3047, 2206 cm^{-1}; ^1H NMR (400 MHz, DMSO-d_6) δ 7.26-8.38 (m, 15H, ArH, NH_2 & pyridine-H), 9.27 (s, 1H, pyrazole-5-H); MS *m/z* (%) 452 (M^+). Anal. Calcd for $C_{27}H_{16}N_8$: C, 71.67; H, 3.56; N, 24.76. Found: C, 71.39; H, 3.45; N, 24.57%.

9-Amino-7-[1-phenyl-3-(thien-2-yl)-1*H*-pyrazol-4-yl]imidazo[1,2-*a*:5,4-*b*']dipyridine-6,8-dicarbonitrile (22b). Brown crystals (325 mg, 71%); mp > 300 °C; IR (KBr) *v* 3535, 3332, 2214 cm^{-1}; ^1H NMR (400 MHz, DMSO-d_6) δ 6.98-9.12 (m, 13H, ArH, NH_2, thiophene-H & pyridine-H), 9.25 (s, 1H, pyrazole-H); MS *m/z* (%) 458 (M^+). Anal. Calcd for $C_{25}H_{14}N_8S$: C, 65.49; H, 3.08; N, 24.44; S, 6.99. Found: C, 65.39; H, 2.95; N, 24.23; S, 6.76%.

Synthesis of 2-(3*H*-imidazo[4,5-*b*]pyrid-2-yl)-3-phenylacrylonitrile (20)

To a mixture of benzaldehyde (**18**) (106 mg, 1 mmol) and 2-(3*H*-imidazo[4,5-*b*]pyrid-2-yl)acetonitrile (**10**) (1 mmol, 110 mg) in absolute EtOH (15 mL) was added piperidine (1 mmol, 110 μL), and the mixture was heated at reflux for 3 h. The crude solid was isolated and recrystallized from DMF/EtOH (25:75) to give **20** as brown crystals, 234 mg (95%); mp 260-262 °C; IR (KBr) *v* 3435, 3055, 2214, cm^{-1}; ^1H NMR (400 MHz, DMSO-d_6) δ 7.30 (dd, 1H, pyridine-3-H, J_1 8.0 Hz, J_2 4.8 Hz), 7.61-8.41 (m, 7H, ArH, pyridine-2-H & pyridine-4-H), 8.44 (s, 1H, =CH-Ph), 13.98 (s,1H, NH); MS *m/z* (%) 246 (M^+). Anal. Calcd for $C_{15}H_{10}N_4$: C, 73.16; H, 4.09; N, 22.75. Found: C, 72.93; H, 3.97; N, 22.55%.

General procedure for the synthesis of bis(2-(3*H*-imidazo[4,5-*b*]pyrid-2-yl)acrylonitrile) derivatives 25a-d

To a mixture of appropriate bis(arylidenemalononitrile) **23a-d** (1 mmole) and 2-(3*H*-imidazo[4,5-*b*]pyrid-2-yl)acetonitrile (**10**) (2 mmol, 316 mg) in absolute EtOH (15 mL) was added piperidine (2 mmol, 110 μL), and the mixture was heated at reflux for 2 h. The crude solid was isolated and recrystallized from DMF/EtOH (25:75) to give **25a-d**, respectively.

2,2'-{3,3'-[Ethane-1,2-diylbis(oxy)]bis(2,1-phenylene)}bis[2-(3*H*-imidazo[4,5-*b*]pyrid-2-yl)acrylonitrile] (25a). Yellow crystals (478 mg, 87%); mp 259-262 °C; IR (KBr) *v* 3433, 3047, 2970, 2214, 1249 cm^{-1}; ^1H NMR (400 MHz, DMSO-d_6) δ 4.63 (s, 4H, OCH_2), 7.06-8.38 (m, 14H, ArH & pyridine-H), 8.59 (s, 2H, 2CH), 13.63 (br. s, 2H, NH); ^{13}C NMR (100 MHz, DMSO-d_6) δ 68.1, 103.4, 104.5, 113.8, 114.6, 116.3, 119.0, 121.6, 122.3, 125.0, 128.9, 133.9, 142.4, 145.1, 149.6, 157.8; MS *m/z* (%) 550 (M^+). Anal. Calcd for $C_{32}H_{22}N_8O_2$: C, 69.81; H, 4.03; N, 20.35. Found: C, 69.55; H, 3.90; N, 20.18%.

2,2'-{3,3'-[Propane-1,3-diylbis(oxy)]bis(2,1-phenylene)}bis[2-(3*H*-imidazo[4,5-*b*]pyrid-2-yl)acrylonitrile] (25b). Pale yellow crystals (508 mg, 90%); mp 268-270 °C; IR (KBr) *v* 3417, 3055, 2954, 2214, 1249 cm^{-1}; ^1H NMR (400 MHz, DMSO-d_6) δ 2.39 (br. s, 2H, CH_2), 4.38 (t, 4H, OCH_2, *J* 6.4 Hz), 7.07-8.40 (m, 14H, ArH &

pyridine-H), 8.62 (s, 2H, 2CH), 13.34 (br. s, 2H, 2NH); MS *m/z* (%) 564 (M^+). Anal. Calcd for $C_{33}H_{24}N_8O_2$: C, 70.20; H, 4.28; N, 19.85. Found: C, 69.92; H, 4.10; N, 19.64%.

2,2'-{3,3'-[Propane-1,3-diylbis(oxy)]bis(4,1-phenylene)}bis[2-(3*H*-imidazo[4,5-*b*]pyrid-2-yl)acrylonitrile] (25c). Yellow crystals (468 mg, 83%); mp 272-274 °C; IR (KBr) *v* 3464, 3047, 2954, 2214, 1257 cm^{-1}; ^{1}H NMR (400 MHz, DMSO-d_6) δ 2.25-2.33 (m, 2H, CH_2), 4.30 (t, 4H, OCH_2, *J* 6.0 Hz), 7.21-8.38 (m, 14H, ArH & pyridine-H), 8.38 (s, 2H, 2CH), 12.38 (br. s, 2H, 2NH); ^{13}C NMR (100 MHz, DMSO-d_6) δ 28.8, 65.1, 99.3, 115.5, 116.0, 116.8, 119.0, 125.6, 132.3, 132.6, 145.0, 146.8, 150.7, 162.0; MS *m/z* (%) 564 (M^+). Anal. Calcd for $C_{33}H_{24}N_8O_2$: C, 70.20; H, 4.28; N, 19.85. Found: C, 70.04; H, 4.09; N, 19.74%.

2,2'-{3,3'-[Butane-1,4-diylbis(oxy)]bis(4,1-phenylene)}bis[2-(3*H*-imidazo[4,5-*b*]pyrid-2-yl)acrylonitrile] (25d). Yellow crystals (543 mg, 94%); mp 267-270 °C; IR (KBr) *v* 3446, 3047, 2954, 2214, 1257 cm^{-1}; ^{1}H NMR (400 MHz, DMSO-d_6) δ 1.93 (br. s, 4H, $2CH_2$), 3.4 (br. s, 2H, 2NH); 4.18 (br. s, 4H, $2CH_2$), 7.10-8.37 (m, 14H, ArH & pyridine-H), 8.37 (s, 2H, 2CH), MS *m/z* (%) 578 (M^+). Anal. Calcd for $C_{34}H_{26}N_8O_2$: C, 70.58; H, 4.53; N, 19.37. Found: C, 70.44; H, 4.30; N, 19.22%.

Computational Details

Due to the absence of single crystal X-ray structure analysis and to attain the molecular conformation of compounds **10**, **11** and **12**, energy minimization analyses were done by means of Gaussian-09W software package.[39] The ground state geometrical structure of the three compounds were optimized using DFT method[40] with the B3LYP exchange correlation functional approach.[41] The basis set 6-311G** was applied for C, H and N atoms.[42] Without any symmetry constraints, the geometry of the investigated systems was totally optimized in gas-phase. Gauss View 5 software[43] was used to create figures of molecular orbitals (MOs). The quantum chemical parameters of the studied compounds are gained from calculations as energies of the lowest unoccupied molecular orbital (E_{LUMO}), the highest occupied molecular orbital (E_{HOMO}), HOMO-LUMO energy gap, E_g, absolute electronegativities, χ, chemical potentials, π, absolute hardness, η, absolute softness, σ, global electrophilicity, ω, global softness, S, and additional electronic charge, ΔN_{max}. These parameters are calculated using the following equations;[44] $E_g = E_{LUMO} - E_{HOMO}$, $\chi = -E_{HOMO} + E_{LUMO}/2$, $\eta = E_{LUMO} - E_{HOMO}/2$, $\sigma = 1/\eta$, $\pi = -\chi$, $S = 1/2\eta$, $\omega = \pi^2/2\eta$ and $\Delta N_{max.} = -\pi/\eta$. The spin density difference map calculations were also achieved to clarify their optical properties. Natural bond orbital (NBO) calculations were done[45] with the NBO code contained in Gaussian 09 to understand different second order interaction between the filled orbital of one subsystem and empty orbital of another subsystem which is the calculate of the molecular delocalization or hyperconjugation. The total static dipole moment (μ), the mean polarizability $\langle\alpha\rangle$, the anisotropy of the polarizability, $\Delta\alpha$ and the mean first-order hyperpolarizability, $\langle\beta\rangle$ using the *x*, *y*, *z* components were calculated by using the following equations at B3LYP/ GENECP level of theory:[46]

$$\mu = (\mu^2_x + \mu^2_y + \mu^2_z)^{1/2},$$

$$\langle\alpha\rangle = 1/3\ (\alpha_{xx} + \alpha_{yy} + \alpha_{zz}),$$

$$\Delta\alpha = ((\alpha_{xx} - \alpha_{yy})^2 + (\alpha_{yy} - \alpha_{zz})^2 + (\alpha_{zz} - \alpha_{xx})^2/2)^{1/2},$$

$$\langle\beta\rangle = (\beta^2_x + \beta^2_y + \beta^2_z)^{1/2},$$

where

$$\beta_x = \beta_{xxx} + \beta_{xyy} + \beta_{xzz},$$

$$\beta_y = \beta_{yyy} + \beta_{xxy} + \beta_{yzz},$$

$$\beta_z = \beta_{zzz} + \beta_{xxz} + \beta_{yyz}.$$

Supplementary Material

^{1}H and ^{13}C NMR spectra for compounds **12a**-**e**; **20**; **22a**,**b** and **25a**-**d** and the tables and figures for the calculation section can be found via the "Supplementary Content" section of this article's webpage.

References

1. Ghanem, N. M.; Farouk, F.; George, R. F.; Abbas, S. E. S.; El-Badry, O. M. *Bioorg. Chem.* **2018**, *80*, 565. https://doi.org/10.1016/j.bioorg.2018.07.006
2. Anaflous, A.; Benchat, N.; Mimouni, M.; Abouricha, S.; Ben-Hadda, T.; El-Bali, B.; Hakkou, A.; Hacht, B. *Lett. Drug Des. Discov.* **2005**, *1*, 224. https://doi.org/10.2174/1570180043398885
3. Marie Kirwen, E.; Batra, T.; Karthikeyan, C.; Deora, G. S.; Rathore, V.; Mulakayala, C.; Mulakayala, N.; Nusbaum, A. C.; Chen, J.; Amawi, H.; et al. *Acta Pharm. Sin. B* **2017**, *7*, 73. https://doi.org/10.1016/j.apsb.2016.05.003
4. Hartwich, A.; Zdzienicka, N.; Schols, D.; Andrei, G.; Snoeck, R.; Głowacka, I. E. *Nucleosides, Nucleotides Nucleic Acids* **2020**, *39*, 542. https://doi.org/10.1080/15257770.2019.1669046
5. Cundy, D. J.; Holan, G.; Otaegui, M.; Simpson, G. W. *Bioorg. Med. Chem. Lett.* **1997**, *7*, 669. https://doi.org/10.1016/S0960-894X(97)00082-6
6. Katritzky, A. R.; Tymoshenko, D. O.; Monteux, D.; Vvedensky, V.; Nikonov, G.; Cooper, C. B.; Deshpande, M. *J. Org. Chem.* **2000**, *65*, 8059. https://doi.org/10.1021/jo000946r
7. Li, Y.; Huang, J. H.; Wang, J. L.; Song, G. T.; Tang, D. Y.; Yao, F.; Lin, H. K.; Yan, W.; Li, H. Y.; Xu, Z. G.; et al. *J. Org. Chem.* **2019**, *84*, 12632. https://doi.org/10.1021/acs.joc.9b01385
8. Musiu, S.; Leyssen, P.; Froeyen, M.; Chezal, J. M.; Neyts, J.; Paeshuyse, J. *Antiviral Res.* **2016**, *129*, 99. https://doi.org/10.1016/j.antiviral.2016.03.007
9. Tokoroyama, T. *Eur. J. Org. Chem.* **2010**, *2010*, 2009. https://doi.org/10.1002/ejoc.200901130
10. Reyes, E.; Uria, U.; Vicario, J. L.; Carrillo, L. *The Catalytic, Enantioselective Michael Reaction*; John Wiley & Sons, Inc.: Hoboken, NJ, USA, 2016. https://doi.org/10.1002/0471264180.or090.01
11. Sapale, S. R.; Borade, N. A. *Eur. J. Mol. Clin. Med.* **2020**, *7*, 4529.
12. Jadhav, S. D.; Ramasami, P.; Sekar, N. *Phys. Sci. Rev.* **2019**, *4*, 32. doi. org/10.1515/psr . https://doi.org/10.1515/psr-2018-0032
13. Nagarajan, N.; Velmurugan, G.; Prakash, A.; Shakti, N.; Katiyar, M.; Venuvanalingam, P.; Renganathan, R. *Chem. Asian J.* **2014**, *9*, 294. https://doi.org/10.1002/asia.201301061
14. Leopoldo, M.; Lacivita, E.; Passafiume, E.; Contino, M.; Colabufo, N. A.; Berardi, F.; Perrone, R. *J. Med. Chem.* **2007**, *50*, 5043. https://doi.org/10.1021/jm070721

15. Abdelmoniem, A. M.; Ghozlan, S. A. S.; Abdelmoniem, D. M.; Elwahy, A. H. M.; Abdelhamid, I. A. *J. Heterocycl. Chem.* **2017**, *54*, 2844. https://doi.org/10.1002/jhet.2890
16. Abdelhamid, I. A.; Darwish, E. S.; Nasra, M. A.; Abdel-Gallil, F. M.; Fleita, D. H. *Synthesis* **2010**, 1107. https://doi.org/10.1055/s-0029-1219235
17. Abdella, A. M.; Mohamed, M. F.; Mohamed, A. F.; Elwahy, A. H. M.; Abdelhamid, I. A. *J. Heterocycl. Chem.* **2018**, *55*, 498. https://doi.org/10.1002/jhet.3072
18. Elnagdi, M. H.; Al-Awadi, N. A.; Abdelhamid, I. A. *Adv. Heterocycl. Chem.* **2009**, *97*, 1. https://doi.org/10.1016/S0065-2725(08)00201-8
19. Salem, M. E.; Darweesh, A. F.; Farag, A. M.; Elwahy, A. H. M. *Tetrahedron* **2016**, *72*, 712. https://doi.org/10.1016/j.tet.2015.12.024
20. Abd El-Fatah, N. A.; Darweesh, A. F.; Mohamed, A. A.; Abdelhamid, I. A.; Elwahy, A. H. M. *Tetrahedron* **2017**, *73*, 1436 . https://doi.org/10.1016/j.tet.2017.01.047
21. Elwahy, A. H. M.; Ahmed, M. M.; El-sadek, M. *J. Chem. Res.* **2001**, *2001*, 175. https://doi.org/10.3184/030823401103169540
22. El-Fatah, N. A. A.; Darweesh, A. F.; Mohamed, A. A.; Abdelhamid, I. A.; Elwahy, A. H. M. *Monatsh. Chem.* **2017**, *148*, 2107. https://doi.org/10.1007/s00706-017-2040-7
23. Sanad, S. M. H.; Kassab, R. M.; Abdelhamid, I. A.; Elwahy, A. H. M. *Heterocycles* **2016**, *92*, 910. https://doi.org/10.3987/COM-16-13441
24. Abdelmoniem, A. M.; Salaheldin, T. A.; Abdelhamid, I. A.; Elwahy, A. H. M. *J. Heterocycl. Chem.* **2017**, *54*, 2670. https://doi.org/10.1002/jhet.2867
25. Diab, H. M.; Abdelhamid, I. A.; Elwahy, A. H. M. *Synlett* **2018**, *29*, 1627. https://doi.org/10.1055/s-0037-1609967
26. Sroor, F. M.; Aboelenin, M. M.; Mahrous, K. F.; Mahmoud, K.; Elwahy, A. H. M.; Abdelhamid, I. A. *Arch. Pharm. (Weinheim).* **2020**, *353*, 2000069. https://doi.org/10.1002/ardp.202000069
27. Takeda, K.; Shudo, K.; Okamoto, T.; Kosuge, T. *Chem. Pharm. Bull. (Tokyo).* **1978**, *26*, 2924 . https://doi.org/10.1248/cpb.26.2924
28. Desbois, N.; Chezal, J. M.; Fauvelle, F.; Debouzy, J. C.; Lartigue, C.; Gueiffier, A.; Blache, Y.; Moreau, E.; Madelmont, J. C.; Chavignon, O.; et al. *Heterocycles* **2005**, *65*, 1121. https://doi.org/10.3987/COM-05-10354
29. Zhang, K.; El Bouakher, A.; Levaique, H.; Bignon, J.; Retailleau, P.; Alami, M.; HAMZE, A. *Adv. Synth. Catal.* **2020**, *362*, 3243. https://doi.org/10.1002/adsc.202000553
30. Pan, T.; He, X.; Chen, B.; Chen, H.; Geng, G.; Luo, H.; Zhang, H.; Bai, C. *Eur. J. Med. Chem.* **2015**, *95*, 500. https://doi.org/10.1016/j.ejmech.2015.03.050
31. Dekhane, D. V.; Pawar, S. S.; Gupta, S. V.; Shingare, M. S.; Thore, S. N. *Chin. Chem. Lett.* **2010**, *21*, 519. https://doi.org/10.1016/j.cclet.2009.11.034

32. Lyons, D. M.; Huttunen, K. M.; Browne, K. A.; Ciccone, A.; Trapani, J. A.; Denny, W. A.; Spicer, J. A. *Bioorg. Med. Chem.* **2011**, *19*, 4091. https://doi.org/10.1016/j.bmc.2011.05.013
33. Darweesh, A. F.; Abd El-Fatah, N. A.; Abdelhamid, I. A.; Elwahy, A. H. M.; Salem, M. E. *Synth. Commun.* **2020**, *50*, 2531. https://doi.org/10.1080/00397911.2020.1784436
34. Ghozlan, S. A. S.; Abdelmoniem, A. M.; Butenschön, H.; Abdelhamid, I. A. *Tetrahedron* **2015**, *71*, 1413. https://doi.org/10.1016/j.tet.2015.01.026
35. Lin, Y. Y.; Rajesh, N. P.; Santhana Raghavan, P.; Ramasamy, P.; Huang, Y. C. *Mater. Lett.* **2002**, *56*, 1074. https://doi.org/10.1016/S0167-577X(02)00680-8
36. Singh, K.; Okombo, J.; Brunschwig, C.; Ndubi, F.; Barnard, L.; Wilkinson, C.; Njogu, P. M.; Njoroge, M.; Laing, L.; Machado, M.; et al. *J. Med. Chem.* **2017**, *60*, 1432. https://doi.org/10.1021/acs.jmedchem.6b01641
37. Salem, M. E.; Hosny, M.; Darweesh, A. F.; Elwahy, A. H. M. *Synth. Commun.* **2019**, *49*, 2319. https://doi.org/10.1080/00397911.2019.1620283
38. Salama, S. K.; Darweesh, A. F.; Abdelhamid, I. A.; Elwahy, A. H. M. *J. Heterocycl. Chem.* **2017**, *54*, 305. https://doi.org/10.1002/jhet.2584
39. Frisch, M. J.; Trucks, G. W.; Schlegel, H. B.; Scuseria, G. E.; Robb, M. A.; Cheeseman, J. R.; Scalmani, G.; Barone, V.; Petersson, G. A.; Nakatsuji, H.; et al. *Gaussian 09, Revision A.02*; 2016.
40. Becke, A. D. *J. Chem. Phys.* **1993**, *98*, 5648. https://doi.org/10.1063/1.464913
41. Lee, C.; Yang, W.; Parr, R. G. *Phys. Rev. B* **1988**, *37*, 785. https://doi.org/10.1103/PhysRevB.37.785
42. Frisch, M. J.; Pople, J. A.; Binkley, J. S. *J. Chem. Phys.* **1984**, *80*, 3265. https://doi.org/10.1063/1.447079
43. Dennington, R.; Keith, T.; Millam, J.; Shawnee, K. S. *GaussView Millam. "version 5; Semichem Inc." Shawnee Mission. KS* **2009**.
44. El-Sonbati, A. Z.; Diab, M. A.; El-Bindary, A. A.; Morgan, S. M. *Spectrochim. Acta - Part A Mol. Biomol. Spectrosc.* **2014**, *127*, 310. https://doi.org/10.1016/j.saa.2014.02.037
45. Chocholoušová, J.; Špirko, V.; Hobza, P. *Phys. Chem. Chem. Phys.* **2004**, *6*, 37. https://doi.org/10.1039/B314148A
46. Avci, D. *Spectrochim. Acta - Part A Mol. Biomol. Spectrosc.* **2011**, *82*, 37. https://doi.org/10.1016/j.saa.2011.06.037